

<https://doi.org/10.1038/s43856-025-00905-8>

Genetic surveillance reveals low but sustained malaria transmission with clonal replacement in Sao Tome and Principe

Check for updates

Ying-An Chen^{1,2}, Peng-Yin Ng², Daniel Garcia-Ruiz^{2,3}, Aaron Elliot¹, Brian Palmer¹,
Ronalg Mendes Costa d' Assunção Carvalho⁴, Lien-Fen Tseng⁵, Cheng-Sheng Lee⁶, Kun-Hsien Tsai^{5,7},
Bryan Greenhouse¹ & Hsiao-Han Chang²✉

Abstract

Background Despite efforts to eliminate malaria in Sao Tome and Principe (STP), cases have recently increased. Understanding residual transmission structure is crucial for developing effective elimination strategies.

Methods This study collected surveillance data and generated amplicon sequencing data from 980 samples between 2010 and 2016 to examine the genetic structure of the parasite population.

Results Here we show that the mean multiplicity of infection (MOI) is 1.3, with 11% polyclonal infections, indicating low transmission intensity. Temporal trends of these genetic metrics do not align with incidence rates, suggesting that changes in genetic metrics may not straightforwardly reflect changes in transmission intensity, particularly in low transmission settings where genetic drift and importation have a substantial impact. While 88% of samples are genetically linked, continuous turnover in genetic clusters and changes in drug-resistance haplotypes are observed. Principal component analysis reveals some STP samples are genetically similar to those from Central and West Africa, indicating possible importation.

Conclusions These findings highlight the need to prioritize several interventions, such as targeted interventions against transmission hotspots, reactive case detection, and strategies to reduce the introduction of new parasites into this island nation as it approaches elimination. This study also serves as a case study for implementing genetic surveillance in a low transmission setting.

Plain language summary

Malaria cases in Sao Tome and Principe rose again around 2012 and have stayed low since, but the disease has not been eliminated. To address this, it is important to understand how malaria continues to spread. By analyzing genetic data of malaria parasites, we found that imported cases may bring new genetic types of the parasite into the population. This can lead to further local transmission and changes in the parasite population, such as the spread of drug resistance. Our findings show the importance of reducing imported cases and stopping their spread, as well as focusing on areas with relatively high transmission and using reactive case detection during the later stages of malaria control programs.

Effective interventions have significantly reduced the malaria burden in the Democratic Republic of Sao Tome and Principe (STP), an island nation in the Gulf of Guinea, Central Africa^{1–3}. In recognition of the substantial progress achieved, the World Health Organization (WHO) has included the

country in the E-2025 initiative, aiming to eliminate malaria by the year 2025⁴. Despite being in a pre-elimination phase, the annual incidence rate has consistently remained around 10 cases per 1000 people over 7 years. Moreover, there was a 46% increase in case numbers reported in 2022⁵.

¹EPPIcenter Research Program, Division of HIV, Infectious Diseases and Global Medicine, Department of Medicine, University of California, San Francisco, CA, USA. ²Institute of Bioinformatics and Structural Biology, College of Life Sciences and Medicine, National Tsing Hua University, Hsinchu, Taiwan, ROC. ³Bioinformatics Program, Institute of Statistical Science, Taiwan International Graduate Program, Academia Sinica, Taipei, Taiwan, ROC. ⁴Taiwanese Medical Mission, São Tomé, São Tomé and Príncipe. ⁵Taiwan Anti-Malarial Advisory Mission, São Tomé, São Tomé and Príncipe. ⁶Institute of Molecular and Cellular Biology, College of Life Sciences and Medicine, National Tsing Hua University, Hsinchu, Taiwan, ROC. ⁷Institute of Environmental and Occupational Health Sciences, College of Public Health, National Taiwan University, Taipei, Taiwan, ROC. ✉e-mail: hhchang@life.nthu.edu.tw

These setbacks pose challenges to achieving the E-2025 goal and underscore the necessity of understanding the genetic structure of residual malaria transmission in STP in order to tailor effective elimination strategies.

The main island, Sao Tome, consists of six administrative districts. The majority of cases occur in the capital district, Agua Grande, where ~40% of the population resides¹. Malaria cases are reported year-round, with a slight decline often observed during the dry season from June to early September^{1,6}. Located about 300 km off the coast of Gabon, STP's increase in international tourism and active trade facilitates potential parasite connectivity between STP and other countries in West and Central Africa⁷. However, there has been limited exploration of the role of importation on malaria transmission in STP⁶. Malaria interventions in STP have focused on vector control^{1,8}, passive case surveillance⁶, and/or mass drug administration⁹, but have not included routine collection of travel history or performing reactive case detection, which may be useful strategies for preventing imported malaria and additional onward transmission in low-transmission settings¹⁰.

The current understanding of malaria transmission in STP includes epidemiological findings, the evaluation of intervention effectiveness, and the analysis of specific genes in the local vector (*Anopheles coluzzii*) and the malaria parasite (*Plasmodium falciparum*)^{1,6,11–13}. However, a gap remains due to the lack of integration between epidemiological metadata and genomic information, which is crucial for understanding the structure of residual transmission in STP. With advancements and cost reductions in sequencing technology, an increasing number of countries are adopting genomic surveillance approaches to track transmission dynamics, potential importations, and the spread of drug-resistant parasites^{14–27}. Several genetic metrics have been proposed to estimate malaria transmission, including the multiplicity of infection (MOI—which denotes the number of genetically distinct parasite strains within an individual), within-host relatedness, F_{WH} , and pairwise relatedness between infections^{22,28–33}. Moreover, in settings with low transmission, genetic data can capture changes in circulating parasites that may not be easily detected through traditional epidemiological or clinical measures, thereby providing useful information for elimination efforts^{14,34}.

To understand the genetic structure of residual malaria transmission in STP, we performed amplicon sequencing to obtain the genome-wide genetic dataset of malaria parasites in the country. By integrating parasite genomic data with epidemiological metadata, this study offers spatiotemporal inferences on transmission clusters that can help guide effective malaria control strategies. The fine-scale analysis of genetic metrics and transmission inferences can serve as a valuable case study for applying genetic epidemiology to malaria in a low-transmission setting, particularly as more countries experience transmission declines and approach malaria elimination.

Materials and methods

Ethics statement

The transfer, shipment, and use of malaria dried blood spots (DBS) and encrypted case surveillance data for research analysis in Taiwan were approved by the Centro Nacional de Endemias (CNE) in STP (No. OF°N°20/P°CNE/2016). The DBS were collected as part of routine clinical care, and anonymized residual samples were used in this study. The use of these residual samples for research purposes was approved by the Research Ethics Committee (REC) of National Taiwan University Hospital (NTUH) (No. 201110023RD) and the Research Ethics Review Committee of National Tsing Hua University (NTHU) (No. 11012HM135). Because the samples were not collected specifically for research and posed no additional risk to participants, the requirement for individual informed consent was waived by both the CNE (No. OF°N°20/P°CNE/2016) and the NTUH REC (No. 201110023).

This research was conducted under an agreement between the Taiwan Anti-Malarial Advisory Team, the Ministry of Foreign Affairs, and the CNE in STP. The research priorities and relevance were determined in close collaboration with local partners, who provided input and facilitated

coordination with local departments. The collaboration aimed to support local capacity and malaria control efforts. There were no animal, environmental, or biorisk concerns, nor risks to researchers or participants. Relevant local and regional studies were cited to contextualize our findings^{1–3,6,8,11–13}.

Study materials

A total of 7482 malaria dried blood spots (DBS) from the Central Hospital Ayres de Menezes (HAM) were obtained from a surveillance project conducted by the Taiwan Anti-Malarial Advisory Team in partnership with the Centro Nacional de Endemias (CNE) of STP (Supplementary Fig. 1a). We randomly selected 1629 DBS, evenly distributed across our study period nationwide, ensuring around 20 samples per month from 2010 to 2016. The average sample sizes by year in areas with relatively high and low malaria endemicity were 70 and 5 per district, respectively. The DBS, along with the basic characteristics of patients (including age, gender, onset date, residential district and village, treatment regime, and diagnostic results), were collected from patients who had either visited or reported to HAM and were confirmed positive for *Plasmodium falciparum* infections through microscopy and/or rapid diagnostic tests. The total numbers of samples from six administrative districts, Agua Grande (AG), Me-Zochi (MZ), Lobata (LO), Cantagalo (CT), Lembra (LE), and Principe (PR) were 936 (57%), 375 (23%), 236 (15%), 74 (5%), 6 (0.4%), and 2 (0.1%), respectively. Agua Grande is the capital district. The incidence data used in this study were provided by the Taiwan Anti-Malarial Advisory Team in STP¹.

DNA extraction and qPCR

DNA was extracted from DBS using the Tween-Chelex method described in Teyssier et al.³⁵. The 6-mm disc from the DBS punch underwent two-step washes with 0.5% Tween 20 in 1X PBS and 1X PBS at 4 °C. After removing the wash solution, the DBS disc was covered with 10% Chelex 100 resin in water at 95 °C for 10 min and centrifuged at 15,000 rpm for 10 min. The resulting supernatant, which contained the extracted DNA, was then transferred into a PCR tube and stored at –20 °C.

Parasite density was measured using the *var*ATS qPCR protocol³⁶. DNA extracted from mock DBS with known parasite densities of 1, 10, 100, 1000, and 10,000 parasites/μL served as qPCR standards. Duplicate sets of these standards were used to generate a standard curve for each run, with a linearity (R^2) value exceeding 0.98 being considered a validated run. The parasite densities of the samples were then benchmarked using the established standard curve. A total of 1478 samples were confirmed as positive with quantified parasite densities and were processed for amplicon sequencing.

Amplicon sequencing

The amplification of two pools, comprising 165 diversity amplicons, 38 drug-resistance amplicons (containing 68 important drug-resistance sites), and 38 immune, diagnostic, and species-related amplicons, was obtained using the MAD⁴HaTTeR³⁷, building on a targeting diverse microhaplotypes³⁸ and the CleanPlex library preparation kit from Paragon Genomics, CA, USA³⁹. The two pools were combined and processed through clean-up steps with magnetic beads for each sample. Samples were then pooled together and gel-extracted based on parasite density and the presence of primer dimers. All sample pools underwent quality checks on a TapeStation (Agilent, CA, USA) and were sequenced with 150 bp paired-end reads on Illumina sequencers.

For quality assurance, each sample plate included at least one positive control (3D7) and several negative controls randomly placed in each plate to monitor amplification efficiency and detect potential contamination. If the positive controls did not perform well (less than 100 reads per amplicon) or if the negative controls showed more than 10 reads per targeted amplicon on average, the entire plate was discarded and re-prepared until good-quality and contamination-free results were obtained. Out of a total of 19 96-well plates used for library construction, two were heavily contaminated, with all negative controls showing average reads ≥10, and four plates exhibited

partial contamination, with 10–30% of negative controls showing average reads ≥ 10 .

Bioinformatic pipeline and quality filtering

The amplicon data were processed through the allele calling pipeline V0.1.8 (available at <https://github.com/EPPIcenter/mad4hatter>). The pipeline consists of core modules designed to filter and correct demultiplexed reads, remove adapters, and enable accurate and precise identification of variant alleles. In this study, we focused on genetic diversity analysis using 165 diversity amplicons to estimate parasite genetic metrics and seven drug-resistance amplicons to infer drug-resistance haplotypes.

To ensure data quality, we applied the following criteria to select high-quality samples for analyses using diversity amplicons: (a) total reads per sample exceeding the number of amplified amplicons multiplied by 100, (b) amplicon coverage exceeding 75%, and (c) more than half of the amplicons having 100 or more reads (Supplementary Fig. 2). These standards ensured uniform and adequate amplification across most amplicons per sample. For drug-resistance amplicons, the criterion was that more than half of them should have 10 or more reads. A total of 980 samples met these requirements and were included in the analysis (Supplementary Fig. 1b). These samples were consistently distributed across the study period from 2010 to 2016, with an average of 13 samples per month nationwide. The sample counts by district were as follows: AG: 545 (56%), MZ: 225 (23%), LO: 158 (16%), CT: 47 (5%), LE: 3 (0.3%), and PR: 2 (0.2%). This distribution closely resembled that of the initial randomly selected sample set ($N = 1629$).

Analysis of parasite genetic diversity

We utilized the *MOIRE* V3.1.0 R package to implement a Bayesian approach for estimating MOI from polyallelic data, accounting for experimental error²⁸. We also estimated a new metric of diversity, the effective MOI (eMOI), by adjusting the true MOI for underlying within-host relatedness (r_w), the average proportion of the genome that is identical by descent across all strains within the same host²⁸. The eMOI was defined as $(\text{MOI} - 1) * (1 - r_w) + 1$. We used the means from the posterior distributions of MOI, eMOI, and r_w as their point estimates. A polyclonal infection was defined as having eMOI greater than 1.1.

We employed the *Dcifer* V1.2.0 R package, an identity-by-descent (IBD) method, to estimate between-host relatedness from polyallelic data (r_b)³¹. Using the *MOIRE*-estimated MOI and allele frequencies as inputs, we obtained an estimation of between-host relatedness for each pair, ranging from 0 to 1, accompanied by a corresponding p value for statistical significance. Genomic clusters were identified by applying various levels of \hat{r}_b , with 0.9 being the default and most stringent threshold and 0.3 being the least. The resulting 62 clusters using the 0.9 threshold were then ordered and named by their size (from small to large; C1 to C62). The clustering network was visualized, displaying only the links with a significance level that had a Bonferroni-corrected p value of less than 0.05.

Given the seasonality of malaria transmission in STP, we classified annual seasons based on the cycle of transmission intensity (Supplementary Table 1 and Supplementary Fig. 3) instead of using the calendar year. The year was categorized from the beginning of the rainy season to the conclusion of the dry season, that is, from September of the prior year to August of the current year. Malaria incidence rates were also calculated based on the adjusted year and geographical groups (Capital or Others). Regression analysis was employed to identify the relationship between MOI, eMOI, and polyclonal infections and other characteristics, including the sampling year, season (rainy or dry), residential area (Capital or Others), location (Q1 and Q2, where Q1 represents locations at the village administrative level with malaria case numbers ranking in the top 25% and Q2 represents others), age, gender, parasite density from qPCR (\log_{10} transformed), and treatment regime (artemisinin-based combination therapy or quinine).

Estimation of effective population size

We estimated the effective population sizes based on temporal changes in allele frequencies between consecutive years using the temporal method in

NeEstimator V2.1^{40–42}. We used SNPs from diversity amplicons and excluded those with more than 50% missing data. Since the generation time for malaria parasites in STP was not previously estimated, we considered scenarios of 2, 5, and 9 generations per year.

Analysis of drug-resistance mutations

A total of 9 amino acid sites across 3 resistance genes (*mdr1*, *dhfr*, and *dhps*) were analyzed. For each sample, we first identified the predominant amino acid at each site using read counts, then combined the major amino acids from six sites in *dhfr* and *dhps* and three sites in *mdr1* (Supplementary Table 2) to determine the drug-resistance haplotype for SP (sulfadoxine-pyrimethamine) and ASAQ/AL (artesunate-amodiaquine/artemether-lumefantrine), respectively.

Principal component analysis (PCA)

We performed PCA for sequences from STP and six African countries, including Gabon, Nigeria, Ghana, Cameroon, Tanzania, and Kenya. Sequences from six African countries were obtained from the *Plasmodium falciparum* genomic variation dataset version 7 (Pf7)⁴³. For each sample, sequences in the regions corresponding to the genomic locations of the diversity amplicons from STP samples were extracted using *BCFtools*⁴⁴. These sequences were then merged with STP amplicon sequences to create a unified dataset. For STP samples with more than one sequence per amplicon per sample, the sequence with the highest read count was used. The concatenated sequences were aligned using the long sequence aligner *FAME*⁴⁵. Sites with homology greater than 90% and sites containing more than 50% gaps were removed. To perform PCA⁴⁶, aligned sequences were converted into a Pandas DataFrame, and bases were one-hot encoded using a base map.

Reporting summary

Further information on research design is available in the Nature Portfolio Reporting Summary linked to this article.

Results

Genetic metrics were consistent with low malaria transmission but did not temporally track with incidence rate

With 980 sequenced samples collected nationwide over 7 consecutive years (Supplementary Fig. 1b and Supplementary Table 1), we examined four genetic metrics related to transmission intensity: MOI (multiplicity of infection), eMOI (effective MOI), within-host relatedness (\hat{r}_w), and the proportion of polyclonal infections. Overall, the MOI and eMOI among the samples were both low (mean = 1.3 [MOI] and 1.08 [eMOI]; Fig. 1a). Monoclonal infections were predominant, with polyclonal infections accounting for only 11% of samples (Fig. 1b). Among polyclonal infections, the average within host relatedness (\hat{r}_w) was high at 0.7 (Q1–Q3 = 0.6–0.8; Fig. 1c). Moreover, the estimated effective population sizes based on allele frequency changes remained below 100 across all years for generation numbers of 2, 5, and 9 per year (Supplementary Fig. 4). Collectively, these data indicating low within-host diversity are consistent with low transmission intensity in STP during the study period. While these genetic metrics varied over time, their temporal trend differed from that of the incidence rate (Spearman's $\rho < 0.6$ and $p > 0.2$ for all; Figs. 1a, b). During the study period, the incidence was highest in 2012, while MOI was higher before and after that (2011 and 2014).

In addition to temporal differences, we identified two other significant factors associated with the proportion of polyclonal infections, MOI, and eMOI (Supplementary Table 3). A higher proportion of polyclonal infections (14% vs. 9%), along with higher MOI (1.34 vs. 1.24) and eMOI (1.10 vs. 1.05), were observed in locations outside or bordering the capital district compared to within the capital (Fig. 2 and Supplementary Table 3). This suggests that effective recombination rates were higher outside or bordering the capital district, despite the fact that the capital district harbored the highest number of malaria cases. Another significant factor was age—individuals aged above 5 years exhibited a higher proportion of polyclonal

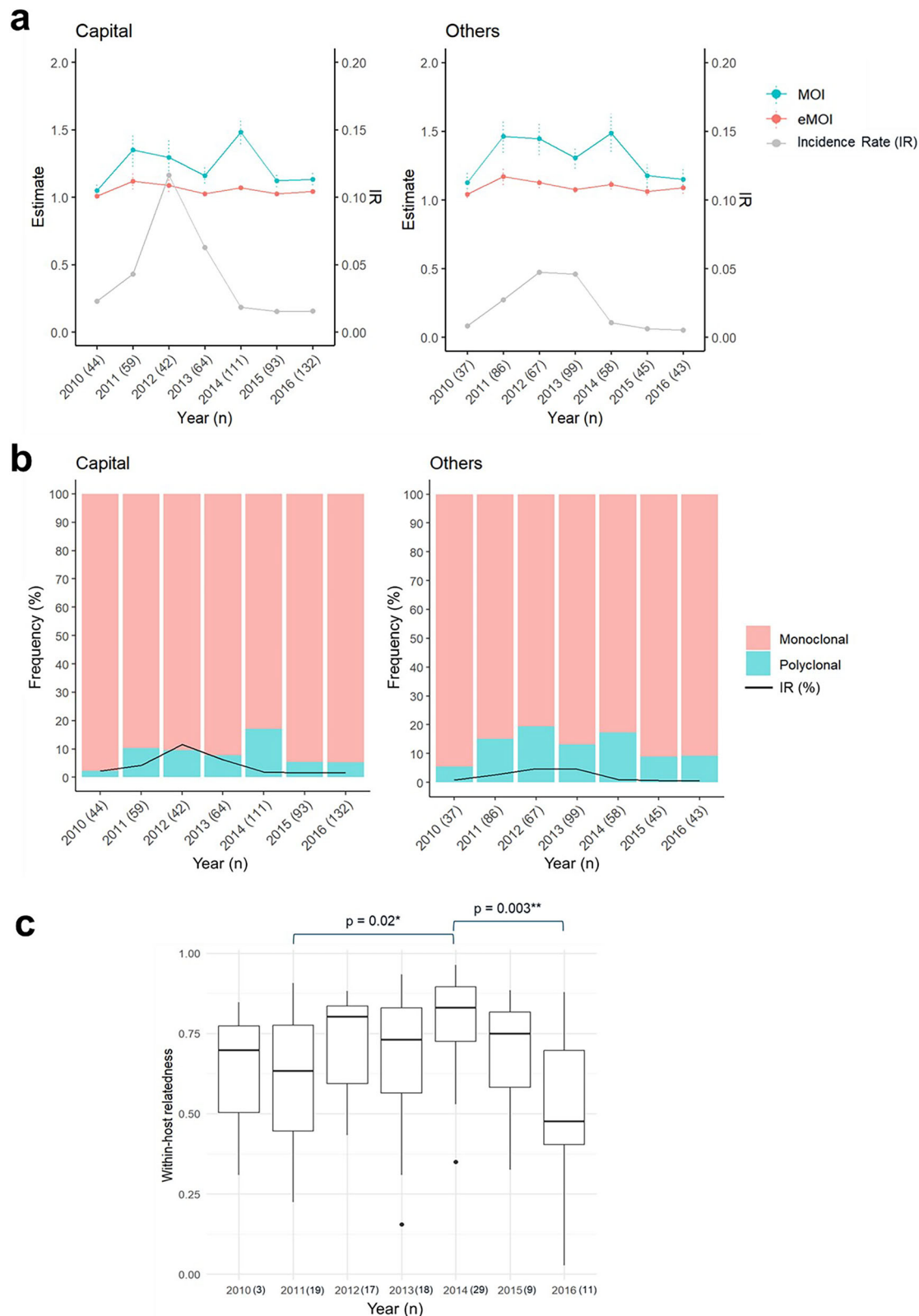
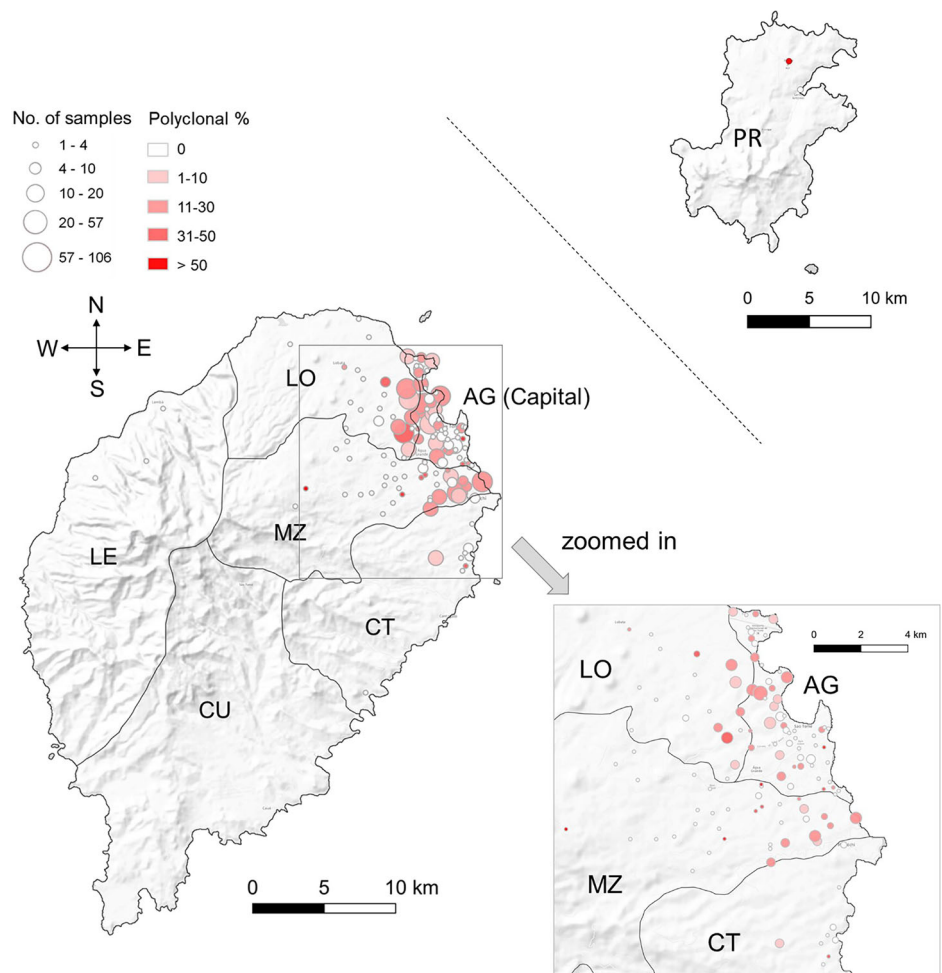


Fig. 1 | Temporal variation of parasite genetic metrics and malaria incidence rates. a Multiplicity of infection (MOI), effective multiplicity of infection (eMOI), and incidence rates (IR) by reclassified year in the capital district (left) and other districts (right). The dots represent the mean for each year, and the bars for MOI and eMOI indicate standard errors. **b** Proportion of polyclonal (cyan) and monoclonal (pink) infections by year. Polyclonal infection is defined as eMOI

greater than 1.1. **c** Boxplot of within-host relatedness (\hat{r}_w) for 106 polyclonal infections across years. Differences in within-host relatedness between years were tested using Dunn's test. The sample size (n) for each year is shown in brackets on the x-axes of (a, b) with a total of 545 samples from the capital district and 435 from other districts.

Fig. 2 | Distribution of sequenced samples and proportion of polyclonal infections. Sao Tome Island comprises six administrative districts: Agua Grande (AG, capital), Lobata (LO), Me-Zochi (MZ), Cantagalo (CT), Caue (CU), and Lemba (LE). Principe (PR) island is located 173 km away from Sao Tome Island. The dots on the map were plotted at the centroids of each location, which may represent residential hamlets, specific places, or roads reported by infected individuals. The size of each dot is proportional to the number of samples sequenced from that location, while the color gradients indicate the level of polyclonal infections.



infections compared to children under 5 (Supplementary Table 3). This trend could be attributed to increased mobility among older individuals, leading to greater exposure to infectious sources. Additionally, a higher proportion of mild or asymptomatic infections among older individuals^{6,47} may result in delayed treatment, facilitating longer duration infections and the potential for superinfection.

Genetic relatedness revealed sustained local transmission with continuous clonal replacement

A large majority of samples (88%) were infected by parasites closely related to at least one other sample (between-host relatedness [\hat{r}_b] ≥ 0.9), forming 62 highly related clusters (Fig. 3a). The high proportion of clustered samples and relatively small number of clusters identified each year (ranging from 8 to 31) suggest that our study captured the majority of a limited extent of population genetic diversity, despite only genotyping a representative sample of cases. In addition, these data suggest that most detected cases resulted from local transmission and, corroborating the incidence and within-host diversity data, are consistent with low transmission intensity. Despite low and seasonal transmission, the majority of clusters (63%) were found across multiple years, indicating sustained local transmission.

While clusters frequently persisted over multiple years, few spanned the entire study period. Generally, we observed turnover in the parasite population over time (Fig. 3a). We found transitional changes in the parasite population over the years across a range of relatedness cutoffs from relaxed ($\hat{r}_b \geq 0.3$) to stringent ($\hat{r}_b \geq 0.9$) (Fig. 4a). Parasites collected in the same year exhibited higher relatedness compared to those collected further apart in time (Fig. 4b). The mean within-year relatedness peaked in 2016 (average

$\hat{r}_b = 0.43$), while the mean between-year relatedness between 2016 and earlier years, such as 2010 or 2011, was very low (average $\hat{r}_b \leq 0.02$) (Fig. 4b). Drug resistance haplotypes also exhibited a temporal trend, with mutations suggesting a decreasing resistance level to SP (Fig. 5a) and an increasing resistance level to AL (Fig. 5b).

Two predominant clusters, C61 and C62, accounted for 17 and 20% of the total samples, respectively, and persisted for 4–5 years, with C61 dominating before 2014 and C62 dominating after 2014 (Figs. 3a and 4c). Upon closer examination, C61 comprises two subgroups, and C62 consists of four subgroups. The samples linking these subgroups were all polyclonal, with MOI values ranging from 2.8 to 4.1 and \hat{r}_w values ranging from 0.26 to 0.5 (Supplementary Fig. 5a). The intra-subgroup \hat{r}_b was very high (mean $\hat{r}_b = 0.99$), contrasting with the very low inter-subgroup \hat{r}_b (mean $\hat{r}_b = 0.03$; Supplementary Fig. 5b). This indicates that the subgroups were largely unrelated, suggesting minimal effective recombination among them. The connector samples among subgroups were likely superinfections, which occurred infrequently and did not produce sufficient recombinants that circulated within the population to be frequently observed. Indeed, when the clustering network was restricted to monoclonal infections, all clusters were clearly separated, with no substructure observed within them (Supplementary Fig. 6). When we lowered the \hat{r}_b cutoff to 0.6, clear substructures remained within C61 and C62, and C61 and C62 became interconnected through few samples that were polyclonal (Fig. 4c). This, along with the low average relatedness between most clusters (Fig. 4d) and the bimodal distribution of within-year \hat{r}_b (Fig. 4e), once again suggests that the parasite clusters in STP were loosely related, with limited yet present opportunities for superinfections and effective recombination, due to low

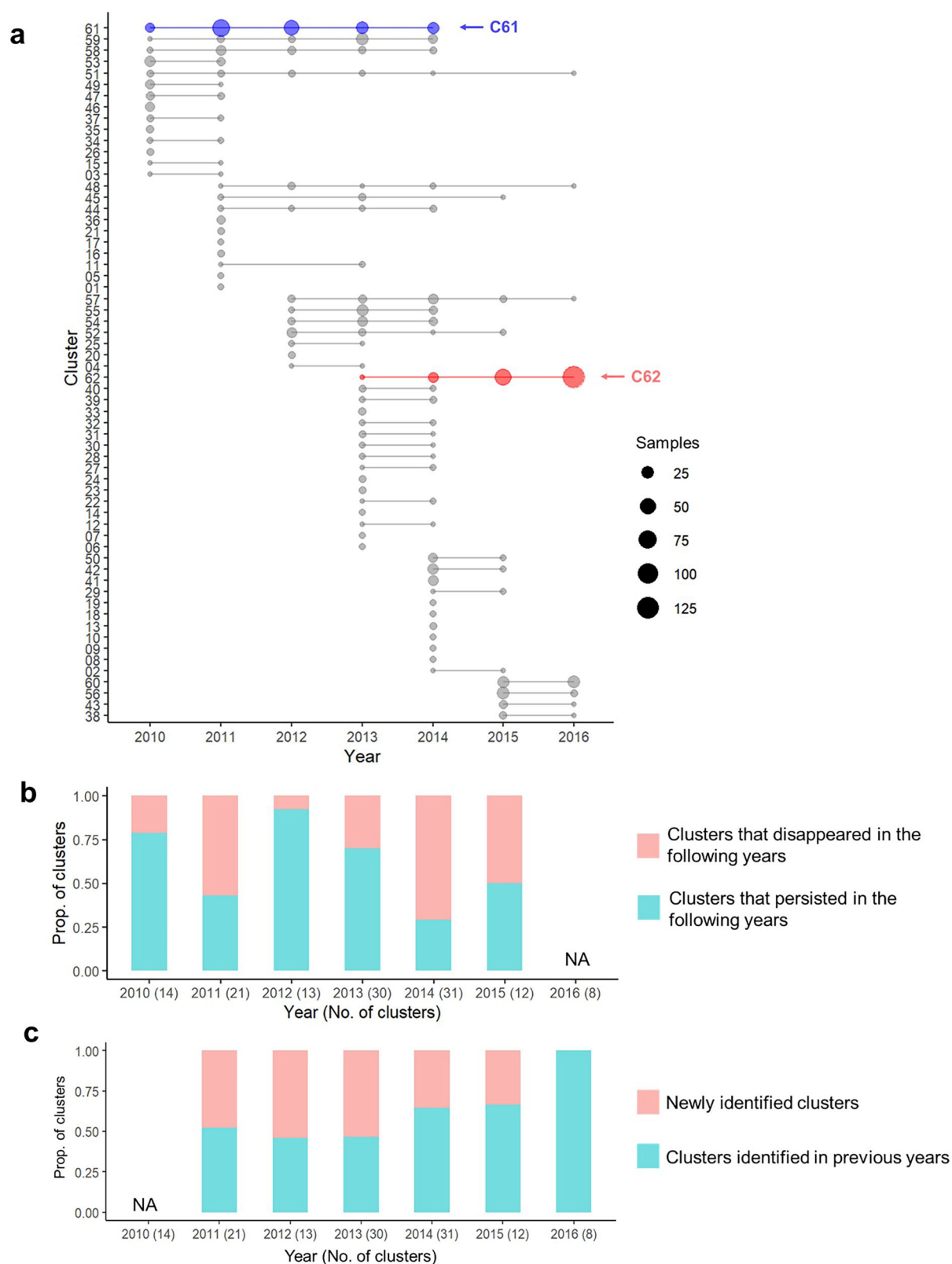


Fig. 3 | Characterization of clusters across years. a Using a cutoff of $\hat{r}_b \geq 0.9$, 62 clusters were identified. The two most prevalent clusters are marked in blue (C61) and red (C62), respectively. **b** Proportion of clusters that disappeared in the following years (pink) and those that persisted (cyan). **c** Proportion of clusters that were

newly identified in each year (pink) and those that were identified in previous years (cyan). NA not applicable (since 2010 is the first year and 2016 is the last year, there is no information for previous years and following years, respectively).

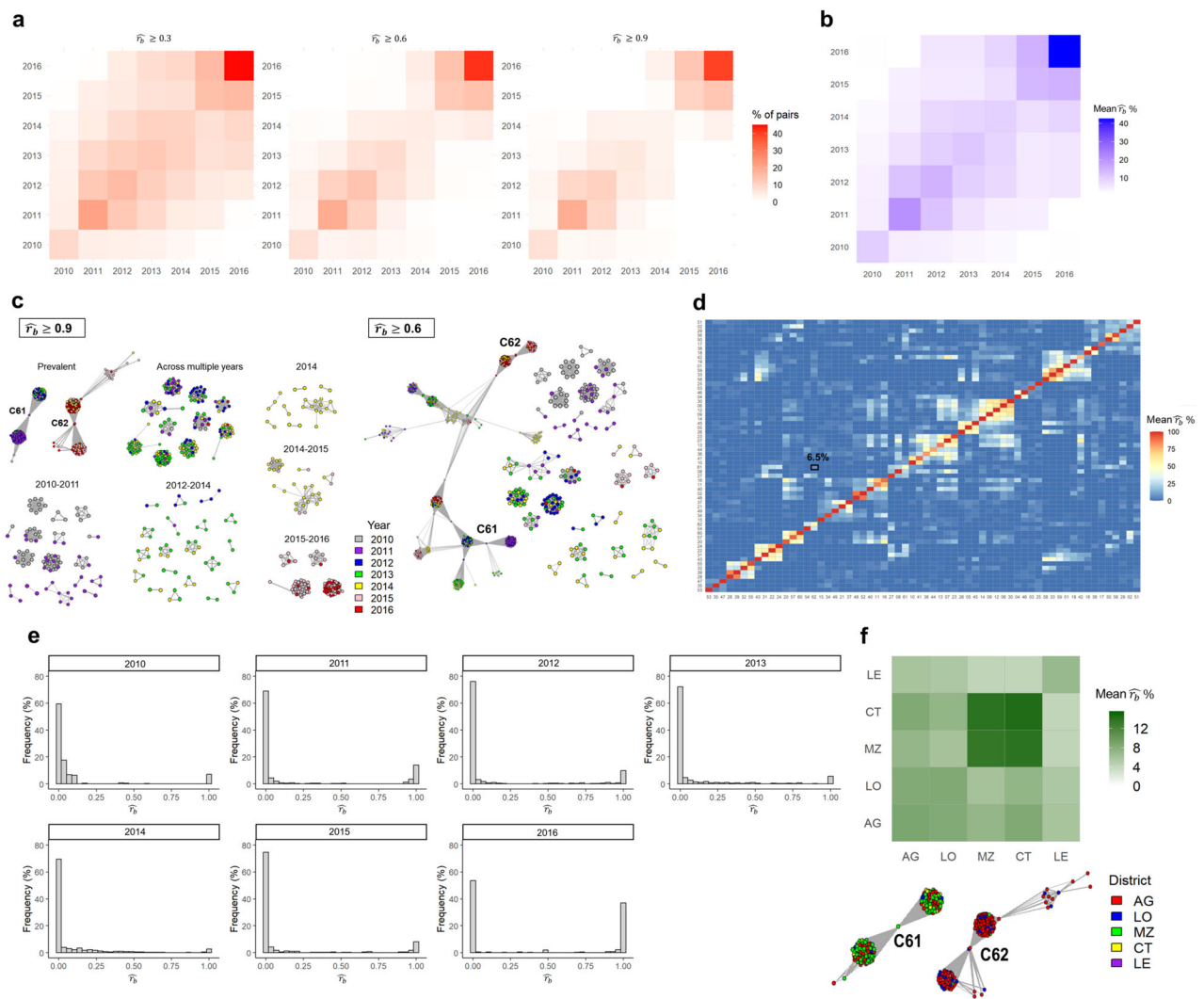


Fig. 4 | Estimated pairwise relatedness across time, space, and clusters.

a Proportion of pairs with \hat{r}_b over 0.3, 0.6, or 0.9 between all pairs of years or within the same years. **b** Mean \hat{r}_b across and within years. **c** Samples with significant relatedness above 0.9 (left) and 0.6 (right) with a Bonferroni-corrected p-value of less than 0.05 are connected. Two predominant clusters, C61 and C62, are connected by

$\hat{r}_b \geq 0.6$ through some transitional infections in 2013 and 2014. **d** Mean \hat{r}_b among 62 clusters identified using $\hat{r}_b \geq 0.9$ cutoff. The average relatedness between C61 and C62 is 6.5% (marked in square). **e** Distribution of \hat{r}_b among samples within the same year. **f** Mean \hat{r}_b between districts in Sao Tome main island and the composition of districts in two predominant clusters, C61 and C62.

transmission intensity. Moreover, consistent with evidence of limited effective recombination, the temporal changes in drug resistance haplotypes were mainly driven by the frequency changes of different sub-clusters to which they belong (Supplementary Fig. 5c).

In addition to temporal changes in the parasite population, we also observed spatial substructure (Fig. 4f). Parasites in or near the capital (AG and LO), where most cases occurred, exhibited similar levels of relatedness within and between districts (average $\hat{r}_b = 0.06\text{--}0.09$). Conversely, two districts with lower incidence rates than the capital, Me-Zochi and Cantagalo, displayed the highest relatedness among themselves (average $\hat{r}_b = 0.13\text{--}0.15$), but lower relatedness with other districts in Sao Tome Island (average $\hat{r}_b \leq 0.09$). While some general spatial substructure was evident, many clusters comprised samples from different districts, including Me-Zochi and Cantagalo, suggesting parasite flow across the entire region (Supplementary Fig. 7). Interestingly, the two predominant clusters, C61 and C62, also exhibited different spatial distributions, with the former mainly existing in AG and MZ, while the latter primarily in AG and LO (Fig. 4f). With the predominant clusters changing from C61 to C62 in 2014, the number of cases in MZ also greatly decreased (Supplementary Fig. 1a), suggesting limited genetic diversity in MZ.

The role of importation and the decreased parasite diversity in the end of the study

Figure 3 illustrates annual turnover in the parasite population, with old clusters disappearing and new clusters emerging. From 2011 to 2015, an average of 45% of clusters (12% of infections) were newly detected each year, representing a substantial amount. The newly emerged clusters may result from newly imported parasites, recombination among pre-existing parasites, and/or an increase in the frequency of infections from previously unsampled clusters. If effective recombination had occurred, we would expect to observe a group of recombinants connecting clusters. However, even after decreasing the \hat{r}_b cutoff to 0.3, the subgroups were connected by few connector samples consistent with superinfections (Supplementary Fig. 8). This suggests a limited role for recombination and a higher likelihood of importation. Additionally, PCA analysis revealed that samples from STP mainly clustered together with samples from Central and West African samples (Fig. 6), suggesting parasite flow between STP islands and other countries in continental Africa. Given that importation is the most likely explanation for the continuous emergence of newly detected clusters, the proportion of samples from these clusters each year (ranging from 7% to

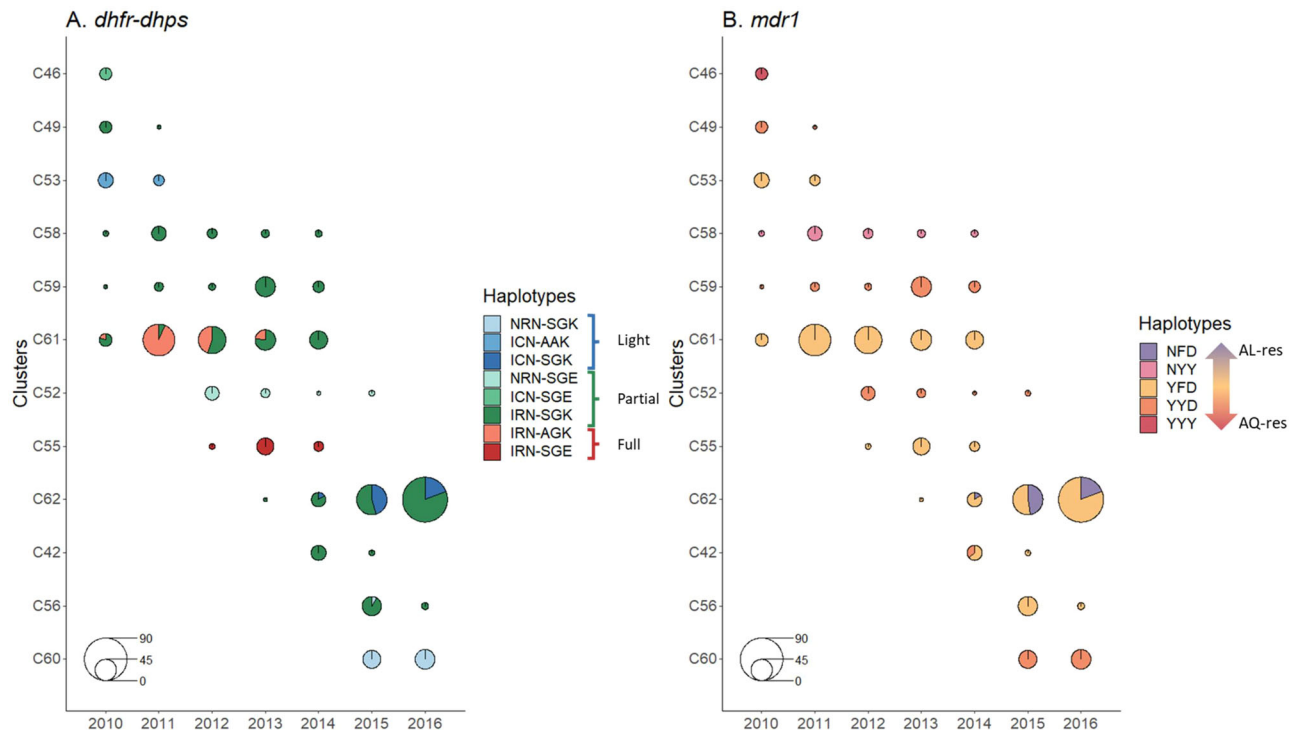


Fig. 5 | Haplotype changes in *dhfr-dhps* and *mdr1* over the years. a The *dhfr-dhps* haplotypes (N511/C59R/S108N-S436A/A437G/K540E) are color-coded according to their resistance levels: blue for light resistance (3 mutants), green for partial resistance (4 mutants), and red for full resistance (5 mutants). **b** The *mdr1* haplotypes (N86Y/Y184F/D1246Y) are colored purple and orange to indicate resistance to

AL and ASAQ, respectively. Following the shift in predominant clusters after 2014, resistance against SP decreased from partial-full (green-red) to light-partial (blue-green). Additionally, the proportion of the AL-resistant haplotype (purple) in *mdr1* haplotypes emerged after 2014.

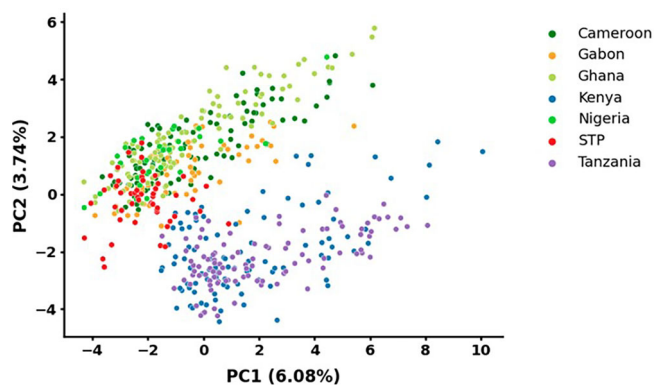


Fig. 6 | Principal component analysis (PCA) of samples from STP and six other African countries. Samples from STP are closely clustered with those from Central and West Africa.

49%, Supplementary Fig. 9) can serve as an upper bound for the impact of importation and subsequent local transmission.

We observed a decline in parasite diversity in the end of the study, reflected by both the number of clusters and parasite effective population size (Figs. 3a and S4). The number of clusters decreased during this period, suggesting that many clusters detected in previous years were either eliminated or reduced in size to undetectable levels (Fig. 3a). The proportion of clusters that were no longer detected in the following years increased after 2014 (Fig. 3b). While newly identified clusters were substantial from 2011 to 2015, a shift was seen in 2016, with no new clusters identified (Fig. 3c). The proportion of non-clustered or uniquely-clustered samples in 2016 was the lowest (7%) across the years, with 74% of the samples belonging to the

predominant cluster C62. These data suggest a decrease in the rate of importation and/or the rates at which imported cases were successfully propagated locally in 2016.

Discussion

Our study investigated the genetic structure of the malaria parasite population in STP using amplicon sequencing technology. To the best of our knowledge, this represents the first genomic description of the parasite population in the country using this approach. We offer a comprehensive depiction of the parasite population dynamics across time and space, capturing the majority of parasite genetic diversity in the country. Our findings reveal sustained, low-level local transmission over a span of 7 years, with moderate turnover of the parasite population likely due to sporadic propagation of imported cases. Given the consistently limited population diversity observed in STP, extending malaria genomic surveillance could serve as a valuable resource for identifying potential cases imported into STP in the future.

Genetic analysis offers valuable insights into parasite population dynamics and the effectiveness of intervention policies, complementing traditional surveillance data such as incidence of malaria^{15,17,22,48–51}. Incidence data may be influenced by health-seeking behaviors, and asymptomatic infections often go undetected. Furthermore, while incidence data provide changes in case numbers over time, they do not reveal the underlying structure of transmission, which is relevant when planning interventions. Our study shows that the majority of infections in STP are closely related to others, suggesting a limited number of parasite lineages circulating in STP. Moreover, while the incidence rate remained similar from 2014 to 2016, genetic analysis revealed that parasite genetic diversity was the lowest in 2016.

This decline may be due to the enhanced malaria control interventions in 2015 and 2016, such as improvements in case management⁶ and the use of new vector control methods, including outdoor larval control and the use

of alternative insecticide in Indoor Residual Spraying (IRS)¹. A similar pattern was observed in Thiès, Senegal, where a decline in malaria incidence was accompanied by reduced genetic diversity, with unique barcodes decreasing by ~50% as incidence dropped^{17,52}. This aligns with our observation in STP, where ~30–50% of the decline in newly identified clusters occurred in 2016, coinciding with the lowest recorded incidence.

After years of malaria control, transmission intensity in several countries or regions, including STP, has decreased to a low level, with the next goal being malaria elimination^{53,54}. In low transmission settings, genetic surveillance plays a crucial role in identifying imported cases⁵⁵, yet questions remain regarding the accuracy of genetic metrics in reflecting changes in underlying transmission levels²⁰. In our study, genetic metrics support the notion of low transmission intensity, but their changes over time, including the proportion of polyclonal infections, MOI, effective MOI, and effective population size, were inconsistent with changes in the incidence rate. While MOI is influenced by transmission intensity, which dictates rates of superinfection and co-transmission, it is also affected by other factors, including host age and immunity, population diversity, importation, and the genetic diversity of the locations from which imported cases originate^{56,57}. Effective population size estimated from allele frequency changes is also influenced by importations, which increase fluctuations in allele frequencies and lead to underestimates in effective population size. In low transmission settings, genetic metrics are highly influenced by stochastic fluctuations in the parasite population. Therefore, caution is warranted when interpreting genetic metrics, and they are better considered in the context of other surveillance data and known or suspected drivers of transmission. Due to the low transmission intensity in STP, the parasite population is particularly susceptible to chance effects, and the continuous emergence of new clusters suggests the impact of importation on genetic metrics. Similarly, recent studies in Senegal and Zambia have also found a limited association between genetic metrics and incidence rates in areas with low transmission intensity^{20,22}.

To establish the genetic basis of malaria parasites in STP, efforts were made to evenly sample across time and space, aiming to reduce bias and capture as many different genetic lineages as possible (Supplementary Fig. 1). We also redefined the boundaries between years based on the transmission season to better reflect changes in malaria transmission from season to season (Supplementary Fig. 3). Utilizing 165 diversity amplicons, we successfully captured both temporal changes and spatial substructure, including the continuous turnover of parasite clusters as well as genetic differentiation between some districts. Additionally, we observed a higher proportion of polyclonal infections outside the capital compared to inside, despite the higher case numbers in the capital. These polyclonal infections from non-capital districts suggest higher rates of transmission leading to superinfection, which provide opportunities for recombination and potentially increase selection efficiency⁵⁸. Given the connectivity between the capital and other districts (Supplementary Fig. 7), these infections have the potential to spread into the capital, thereby complicating malaria control efforts.

Furthermore, evidence of a moderate degree of importation was inferred from the clustering patterns and PCA results. Despite Sao Tome and Principe islands being ~300 km apart from the mainland of Africa, the increased international tourism and frequent trading with high malaria transmission countries like Cameroon, Nigeria, and Gabon in recent years⁷ make it reasonable to expect importation. However, the absence of comprehensive travel surveys has made it difficult to identify imported or introduced cases^{59,60}. Although this study utilized genetic relatedness to understand importation, it could not fully distinguish previously unsampled parasites present in the population from imported parasites. Therefore, incorporating a systematic travel survey, routine reactive case detection, and more comprehensive genomic surveillance into the elimination program could enhance monitoring and support design and evaluation of strategies to reduce the impact of importation^{61–64}.

Our study also characterized changes in drug resistance haplotypes of three genes, *mdr1*, *dhfr*, and *dhps* in STP, revealing a decrease of SP-resistant

haplotypes and an increase in AL-resistant haplotypes. Sulfadoxine-pyrimethamine (SP) is used solely for intermittent preventive treatment (IPT) in pregnancy in STP [2] and its infrequent use may explain the decrease in SP resistance. According to WHO guidance⁶⁵, AL, one of the artemisinin-based combination therapies (ACT), is used as a second-line drug in STP⁶. Among patients in our data, another ACT, AQ, is more frequently used and AL is rarely used. Thus, the increase in resistance to AL is unlikely driven by its use in STP, but is more likely led by the co-occurrence of AL-resistant and SP-lightly-resistant haplotypes in the same subgroups (Supplementary Fig. 5c) and/or other non-selective factors, such as frequency changes of subgroups due to genetic drift or the emergence of new subgroups due to importation. While AL is rarely used in STP, it is recommended for treating uncomplicated infections in nearby countries such as Angola, Gabon, Nigeria, and Cameroon⁵. Treatment failure of AL for uncomplicated *P. falciparum* malaria has been increasingly reported in sub-Saharan African countries^{66–69}. Since the frequency of drug-resistant parasites can change rapidly once they evolve in a low-transmission area, routine surveillance of drug-resistance mutations or haplotypes is crucial in STP.

The last mile for STP to eliminate malaria could be challenging, given the increasing number of cases recorded in the past three years^{5,70}. Our study revealed that the majority of malaria population was infected by highly clonal parasites with sustained transmission, while a minority were attributed to genetically distinct parasites likely originating from external sources. Therefore, we recommend prioritizing the disruption of local transmission, as it reduces the likelihood of sustained local transmission and limits the spread of imported cases. Additionally, we suggest implementing routine reactive surveillance and collecting travel histories, particularly for highly mobile individuals⁷¹. Moreover, this study also demonstrates how genomic surveillance can enhance our understanding of transmission dynamics. Focusing molecular monitoring surveillance efforts on hotspot areas ensures that resources are used more effectively to address critical issues identified in this study, including tracking drug resistance, assessing the impact of imported cases, and monitoring clonal replacement. This is particularly important for low-transmission countries like STP, as it enables the establishment of strong early warning systems and aids in achieving the elimination goal.

Conclusion

Leveraging both genomic and epidemiological data allows us to capture fine-scale dynamics of the parasite population in a pre-elimination setting. In a low-transmission setting, parasites could have experienced significant changes in population structure and drug resistance, as our study demonstrated. Targeted interventions should not only be strengthened in common foci to eliminate prevalent strains but also involve reactive case detection and tracking of travel history to prevent imported transmission in STP.

Data availability

The source data underlying Fig. 6 is provided as Supplementary Data 1. Amplicon sequencing data and associated epidemiological metadata are available in the NCBI Sequence Read Archive (SRA) under accession code PRJNA1237599. Sequencing data was aligned to specific regions of the Pf3D7 genome, using the reference available at https://github.com/EPPICenter/mad4hatter/blob/main/resources/v4/v4_reference.fasta.

Code availability

The analysis code used in this study has been deposited in the GitHub repository and is accessible at https://github.com/hhc-lab/malaria_genetics_STP. The repository is publicly accessible, and no restrictions apply. The exact version of the code used in this study has been archived in Figshare (<https://doi.org/10.6084/m9.figshare.28523960.v1>)⁷². The analysis of parasite genetic diversity was performed using R 4.2.0 with the following packages: *Dcifer* V1.2.0 and *MOIRE* V3.1.0. The estimation of effective population sizes was performed with *NeEstimator* V2.1.

Received: 18 September 2024; Accepted: 9 May 2025;
Published online: 27 May 2025

References

- Chen, Y. A. et al. Effects of indoor residual spraying and outdoor larval control on *Anopheles coluzzii* from São Tomé and Príncipe, two islands with pre-eliminated malaria. *Malar. J.* **18**, 405 (2019).
- Teklehaimanot, H. D., Teklehaimanot, A., Kiszewski, A., Rampao, H. S. & Sachs, J. D. Malaria in Sao Tome and principe: on the brink of elimination after three years of effective antimalarial measures. *Am. J. Trop. Med Hyg.* **80**, 133–140 (2009).
- Wang, Y. et al. Burden of malaria in São Tomé and Príncipe, 1990–2019: findings from the global burden of disease study 2019. *Int. J. Environ. Res. Public Health* **19**, <https://doi.org/10.3390/ijerph192214817> (2022).
- WHO. World Malaria Day: WHO launches effort to stamp out malaria in 25 more countries by 2025. Available from: <https://www.who.int/news/item/21-04-2021-world-malaria-day-who-launches-effort-to-stamp-out-malaria-in-25-more-countries-by-2025> (2021).
- WHO. *World Malaria Report 2023* (World Health Organization, 2023).
- Chen, Y. A. et al. Dynamic changes in genetic diversity, drug resistance mutations, and treatment outcomes of falciparum malaria from the low-transmission to the pre-elimination phase on the islands of São Tomé and Príncipe. *Malar. J.* **20**, 467 (2021).
- Tralac. *São Tomé and Príncipe: 2019 Intra-Africa Trade and Tariff Profile* (Tralac, 2020).
- Tseng, L. F. et al. Rapid control of malaria by means of indoor residual spraying of alphacypermethrin in the Democratic Republic of Sao Tome and Principe. *Am. J. Trop. Med Hyg.* **78**, 248–250 (2008).
- Li, M. et al. Mass drug administration with artemisinin-piperaquine for the elimination of residual foci of malaria in São Tomé Island. *Front. Med.* **8**, 617195 (2021).
- Moonen, B. et al. Operational strategies to achieve and maintain malaria elimination. *Lancet* **376**, 1592–1603 (2010).
- Pinto, J. et al. Genetic structure of *Anopheles gambiae* (Diptera: Culicidae) in Sao Tome and Principe (West Africa): implications for malaria control. *Mol. Ecol.* **11**, 2183–2187 (2002).
- Pinto, J. et al. Malaria in Sao Tome and Principe: parasite prevalences and vector densities. *Acta Trop.* **76**, 185–193 (2000).
- Lee, P. W. et al. Potential threat of malaria epidemics in a low transmission area, as exemplified by São Tomé and Príncipe. *Malar. J.* **9**, 264 (2010).
- Nsanzabana, C. Strengthening surveillance systems for malaria elimination by integrating molecular and genomic data. *Trop. Med. Infect. Dis.* **4**, <https://doi.org/10.3390/tropicalmed4040139> (2019).
- Neafsey, D. E. & Volkman, S. K. Malaria genomics in the era of eradication. *Cold Spring Harb Perspect Med.* **7**, <https://doi.org/10.1101/cshperspect.a025544> (2017).
- Tessema, S. K. et al. Applying next-generation sequencing to track falciparum malaria in sub-Saharan Africa. *Malar. J.* **18**, 268 (2019).
- Daniels, R. et al. Genetic surveillance detects both clonal and epidemic transmission of malaria following enhanced intervention in Senegal. *PLoS ONE* **8**, e60780 (2013).
- Nkhoma, S. C. et al. Population genetic correlates of declining transmission in a human pathogen. *Mol. Ecol.* **22**, 273–285 (2013).
- Hendry, J. A., Kwiatkowski, D. & McVean, G. Elucidating relationships between *P. falciparum* prevalence and measures of genetic diversity with a combined genetic-epidemiological model of malaria. *PLoS Comput. Biol.* **17**, e1009287 (2021).
- Schaffner, S. F. et al. Malaria surveillance reveals parasite relatedness, signatures of selection, and correlates of transmission across Senegal. *Nat. Commun.* **14**, 7268 (2023).
- Carrasquilla, M. et al. Resolving drug selection and migration in an inbred South American *Plasmodium falciparum* population with identity-by-descent analysis. *PLoS Pathog.* **18**, e1010993 (2022).
- Fola, A. A. et al. Temporal and spatial analysis of *Plasmodium falciparum* genomics reveals patterns of parasite connectivity in a low-transmission district in Southern Province, Zambia. *Malar. J.* **22**, 208 (2023).
- Neafsey, D. E., Taylor, A. R. & MacInnis, B. L. Advances and opportunities in malaria population genomics. *Nat. Rev. Genet.* **22**, 502–517 (2021).
- Ruybal-Pesántez, S. et al. Molecular markers for malaria genetic epidemiology: progress and pitfalls. *Trends Parasitol.* **40**, 147–163 (2024).
- Henden, L., Lee, S., Mueller, I., Barry, A. & Bahlo, M. Identity-by-descent analyses for measuring population dynamics and selection in recombining pathogens. *PLoS Genet.* **14**, e1007279 (2018).
- Campino, S. et al. Population genetic analysis of *Plasmodium falciparum* parasites using a customized Illumina GoldenGate genotyping assay. *PLoS ONE* **6**, e20251 (2011).
- Connelly, S. V. et al. Strong isolation by distance and evidence of population microstructure reflect ongoing *Plasmodium falciparum* transmission in Zanzibar. *eLife* **12**, RP90173 (2024).
- Murphy, M. & Greenhouse, B. MOIRE: a software package for the estimation of allele frequencies and effective multiplicity of infection from polyallelic data. *Bioinformatics* **40**, btac619 (2023).
- Nkhoma, S. C. et al. Co-transmission of related malaria parasite lineages shapes within-host parasite diversity. *Cell Host Microbe* **27**, 93–103.e104 (2020).
- Chang, H.-H. et al. THE REAL McCOIL: a method for the concurrent estimation of the complexity of infection and SNP allele frequency for malaria parasites. *PLOS Comput. Biol.* **13**, e1005348 (2017).
- Gerlovina, I., Gerlovin, B., Rodríguez-Barraquer, I. & Greenhouse, B. Dcifer: an IBD-based method to calculate genetic distance between polyclonal infections. *Genetics* **222**, iyac126, <https://doi.org/10.1093/genetics/iyac126> (2022).
- Schaffner, S. F., Taylor, A. R., Wong, W., Wirth, D. F. & Neafsey, D. E. hmmlBD: software to infer pairwise identity by descent between haploid genotypes. *Malar. J.* **17**, 196 (2018).
- Auburn, S. et al. Characterization of within-host plasmodium falciparum diversity using next-generation sequence data. *PLoS ONE* **7**, e32891 (2012).
- Dalmat, R., Naughton, B., Kwan-Gett, T. S., Slyker, J. & Stuckey, E. M. Use cases for genetic epidemiology in malaria elimination. *Malar. J.* **18**, 163 (2019).
- Teyssier, N. B. et al. Optimization of whole-genome sequencing of *Plasmodium falciparum* from low-density dried blood spot samples. *Malar. J.* **20**, 116 (2021).
- Gruenberg, M. et al. Utility of ultra-sensitive qPCR to detect *Plasmodium falciparum* and *Plasmodium vivax* infections under different transmission intensities. *Malar. J.* **19**, 319 (2020).
- Aranda-Diaz, A. et al. Sensitive and modular amplicon sequencing of *Plasmodium falciparum* diversity and resistance for research and public health. *Sci. Rep.* **15**, 10737 (2025).
- Tessema, S. K. et al. Sensitive, highly multiplexed sequencing of microhaplotypes from the plasmodium falciparum heterozygome. *J. Infect. Dis.* **225**, 1227–1237 (2022).
- Paragon Genomics, I. CleanPlex® Targeted Library Preparation User Guide For Amplicon Sequencing on Illumina® Sequencers. https://www.paragongenomics.com/wp-content/uploads/2016/06/CleanPlex-Library-Kit_User_Guide_02111620A1-EN.pdf (2018).

40. Do, C. et al. NeEstimator v2: re-implementation of software for the estimation of contemporary effective population size (N_e) from genetic data. *Mol. Ecol. Resour.* **14**, 209–214 (2014).
41. Jorde, P. E. & Ryman, N. Temporal allele frequency change and estimation of effective size in populations with overlapping generations. *Genetics* **139**, 1077–1090 (1995).
42. Waples, R. S. A generalized approach for estimating effective population size from temporal changes in allele frequency. *Genetics* **121**, 379–391 (1989).
43. Abdel Hamid, M. M. et al. Pf7: an open dataset of Plasmodium falciparum genome variation in 20,000 worldwide samples. *Wellcome Open Res.* **8**, 22 (2023).
44. Li, H. et al. The sequence alignment/map format and SAMtools. *Bioinformatics* **25**, 2078–2079 (2009).
45. Naznooshsadat, E., Elham, P. & Ali, S.-Z. FAME: fast and memory efficient multiple sequences alignment tool through compatible chain of roots. *Bioinformatics* **36**, 3662–3668 (2020).
46. Konishi, T. et al. Principal component analysis applied directly to sequence matrix. *Sci. Rep.* **9**, 19297 (2019).
47. Salgado, C. et al. The prevalence and density of asymptomatic Plasmodium falciparum infections among children and adults in three communities of western Kenya. *Malar. J.* **20**, 371 (2021).
48. Wesolowski, A. et al. Mapping malaria by combining parasite genomic and epidemiologic data. *BMC Med.* **16**, 190 (2018).
49. Chang, H.-H. et al. Mapping imported malaria in Bangladesh using parasite genetic and human mobility data. *eLife* **8**, e43481 (2019).
50. Daniels, R. F. et al. Genetic analysis reveals unique characteristics of Plasmodium falciparum parasite populations in Haiti. *Malar. J.* **19**, 379 (2020).
51. Verity, R. et al. The impact of antimalarial resistance on the genetic structure of Plasmodium falciparum in the DRC. *Nat. Commun.* **11**, 2107 (2020).
52. Daniels, R. F. et al. Modeling malaria genomics reveals transmission decline and rebound in Senegal. *Proc. Natl Acad. Sci. USA* **112**, 7067–7072 (2015).
53. Lindblade, K. A. et al. Supporting countries to achieve their malaria elimination goals: the WHO E-2020 initiative. *Malar. J.* **20**, 481 (2021).
54. Wangmo, L. D. et al. Sustaining progress towards malaria elimination by 2025: lessons from Bhutan & Timor-Leste. *Lancet Reg. Health West Pac.* **22**, <https://doi.org/10.1016/j.lanwpc.2022.100429> (2022).
55. WHO. *Technical Consultation on The Role of Parasite and Anopheline Genetics in Malaria Surveillance* (2019).
56. Roh, M. E. et al. High genetic diversity of Plasmodium falciparum in the low-transmission setting of the Kingdom of Eswatini. *J. Infect. Dis.* **220**, 1346–1354 (2019).
57. Labbé, F. et al. Neutral vs. non-neutral genetic footprints of Plasmodium falciparum multiclonal infections. *PLoS Comput. Biol.* **19**, e1010816 (2023).
58. Rice, W. R. & Chippindale, A. K. Sexual recombination and the power of natural selection. *Science* **294**, 555–559 (2001).
59. Wesolowski, A. et al. Quantifying the impact of human mobility on malaria. *Science* **338**, 267–270 (2012).
60. Ruktanonchai, N. W. et al. Identifying malaria transmission foci for elimination using human mobility data. *PLoS Comput. Biol.* **12**, e1004846 (2016).
61. Hagmann, R. et al. Malaria and its possible control on the island of Principe. *Malar. J.* **2**, 15 (2003).
62. Fakihi, B. S. et al. Risk of imported malaria infections in Zanzibar: a cross-sectional study. *Infect. Dis. Poverty* **12**, 80 (2023).
63. Das, A. M. et al. Modelling the impact of interventions on imported, introduced and indigenous malaria infections in Zanzibar, Tanzania. *Nat. Commun.* **14**, 2750 (2023).
64. Guerra, C. A. et al. Human mobility patterns and malaria importation on Bioko Island. *Nat. Commun.* **10**, 2332 (2019).
65. WHO. *Artemisinin Resistance and Artemisinin-based Combination Therapy Efficacy* (WHO, 2018).
66. Halsey, E. S. & Plucinski, M. M. Out of Africa: increasing reports of artemether-lumefantrine treatment failures of uncomplicated Plasmodium falciparum infection. *J. Travel Med.* **30**, <https://doi.org/10.1093/jtm/taad159> (2023).
67. Silva-Pinto, A. et al. Artemether-lumefantrine treatment failure of uncomplicated Plasmodium falciparum malaria in travellers coming from Angola and Mozambique. *Int. J. Infect. Dis.* **110**, 151–154 (2021).
68. van Schalkwyk, D. A. et al. Treatment failure in a UK Malaria patient harboring genetically variant plasmodium falciparum from uganda with reduced in vitro susceptibility to artemisinin and lumefantrine. *Clin. Infect. Dis.* <https://doi.org/10.1093/cid/ciad724> (2023).
69. Ebong, C. et al. Efficacy and safety of artemether-lumefantrine and dihydroartemisinin-piperaquine for the treatment of uncomplicated Plasmodium falciparum malaria and prevalence of molecular markers associated with artemisinin and partner drug resistance in Uganda. *Malar. J.* **20**, 484 (2021).
70. WHO. *Towards Malaria Elimination: Strengthening the Quality Of Malaria Diagnostic Services in Sao Tome and Principe* (WHO, 2023).
71. Chen, Y.-A. et al. Genomic epidemiology demonstrates spatially clustered, local transmission of Plasmodium falciparum in forest-going populations in southern Lao PDR. *PLoS Pathog.* **20**, e1012194 (2024).
72. Chang, H.-H. malaria_genetics_STP-main. <https://doi.org/10.6084/m9.figshare.28523960.v1> (2025).

Acknowledgements

We would like to express our gratitude to the study participants and study teams for their cooperation, especially the Taiwan Anti-Malarial Advisory Mission and the Centro Nacional de Endemias (CNE) in STP. We also want to express our deepest gratitude to the leader of the Taiwan Anti-Malarial Advisory Mission team, Dr. Jih-Ching Lien, and to Dr. Arlindo Vicente de Assunção Carvalho from the local health ministry. Dr. Jih-Ching Lien (1927–2022) was a leading entomologist who made significant contributions to the identification of mosquito specimens. Dr. Arlindo Vicente de Assunção Carvalho (1961–2024) not only provided professional suggestions for the study but also assisted in coordinating with local departments. We thank Maxwell Murphy and Inna Gerlovina from the UCSF EPPIcenter for their comments on data analysis, Andres Aranda-Diaz for his guidance on the amplicon sequencing experiment and bioinformatic pipeline, and Ju-Hsuan Wang and Yu-Wen Huang for their help with data collection. This research was funded by the Taiwan Ministry of Foreign Affairs and the National Science and Technology Council (NSTC 113-2636-B-007-006). Y.A.C. was supported by the Fulbright Program and the UCSF EPPIcenter. H.H.C. was supported by Yushan Scholar Program. B.G. was supported by NIH/NIAID mentoring award K24 AI144048.

Author contributions

H.H.C., Y.A.C., B.G. and K.H.T. conceptualized the study. R.C., L.F.T. and K.H.T. led the data and sample collection. Y.A.C. and C.S.L. designed and supervised the experiments. Y.A.C., P.Y.N. and A.E. performed experiments. Y.A.C., D.G. and P.Y.N. conducted the analysis. Y.A.C. and B.P. assisted with the bioinformatic analysis. Y.A.C., H.H.C. and B.G. contributed to the interpretation of the results. Y.A.C. and H.H.C. wrote the manuscript with help from P.Y.N., D.G., C.S.L. and B.G..

Competing interests

The authors declare no competing interests.

Additional information

Supplementary information The online version contains supplementary material available at <https://doi.org/10.1038/s43856-025-00905-8>.

Correspondence and requests for materials should be addressed to Hsiao-Han Chang.

Peer review information *Communications Medicine* thanks the anonymous reviewers for their contribution to the peer review of this work. A peer review file is available.

Reprints and permissions information is available at <http://www.nature.com/reprints>

Publisher's note Springer Nature remains neutral with regard to jurisdictional claims in published maps and institutional affiliations.

Open Access This article is licensed under a Creative Commons Attribution-NonCommercial-NoDerivatives 4.0 International License, which permits any non-commercial use, sharing, distribution and reproduction in any medium or format, as long as you give appropriate credit to the original author(s) and the source, provide a link to the Creative Commons licence, and indicate if you modified the licensed material. You do not have permission under this licence to share adapted material derived from this article or parts of it. The images or other third party material in this article are included in the article's Creative Commons licence, unless indicated otherwise in a credit line to the material. If material is not included in the article's Creative Commons licence and your intended use is not permitted by statutory regulation or exceeds the permitted use, you will need to obtain permission directly from the copyright holder. To view a copy of this licence, visit <http://creativecommons.org/licenses/by-nc-nd/4.0/>.

© The Author(s) 2025